Supplemental Figures Verdegaal et al

Supplemental Figure S1.
Immunophenotyping of infused TIL.
Administered TIL were stained with antibody panels specific for regulatory T cell markers (t); see details in supplemental Table 2. High-dimensional single cell data analysis of the stained TIL were performed by opt-distributed Stochastic Neighbor Embedding (optSNE) and FLOWSOM using OMIQ software resulting in the definition of 13 different clusters (t_1 thru t_13) (see main text Figure 2A-D). (A) Contour plots show the staining intensity of the individual markers used. (B) Frequencies of populations t_2 thru t_9 and t_11 thru t_13 are shown as percentage of total TIL for patients with a shorter (short) or longer (long) than median PFS, respectively. (C) Similarly, frequencies of populations t_2 thru t_9 and t_11 thru t_13 are shown as percentage of total TIL for patients with a shorter (short) or longer (long) than median OS, respectively. No statistical differences were observed by Mann-Whitney.

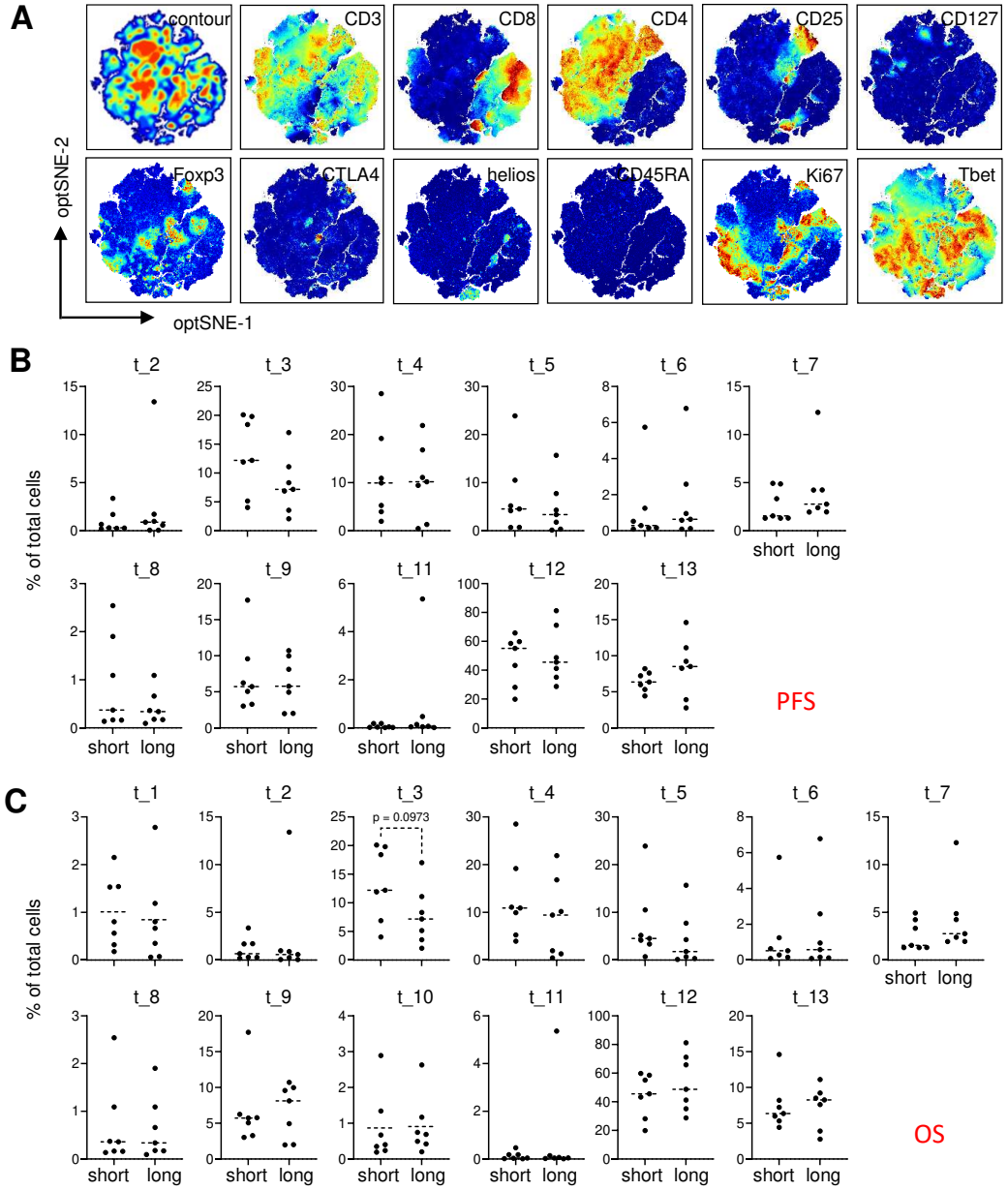

Supplemental Figure S2.
Immunophenotyping of infused TIL.
Administered TIL were stained with antibody panels specific for inhibitory/activation markers (i) see details in supplemental Table 2. Using opt-SNE, FLOWSOM and OMIQ software 14 different clusters (i_1 thru i_14) were defined (see main text Figure 2E-H). (A) Contour plots show the staining intensity of the individual markers used. (B) Frequencies of populations i_1 and i_3 thru i_14 are shown as percentage of total TIL for patients with a shorter (short) or longer (long) than median PFS, respectively. (C) Similarly, frequencies of populations i_1 and i_3 thru i_14 are shown as percentage of total TIL for patients with a shorter (short) or longer (long) than median OS, respectively. No statistical differences were observed by Mann-Whitney.

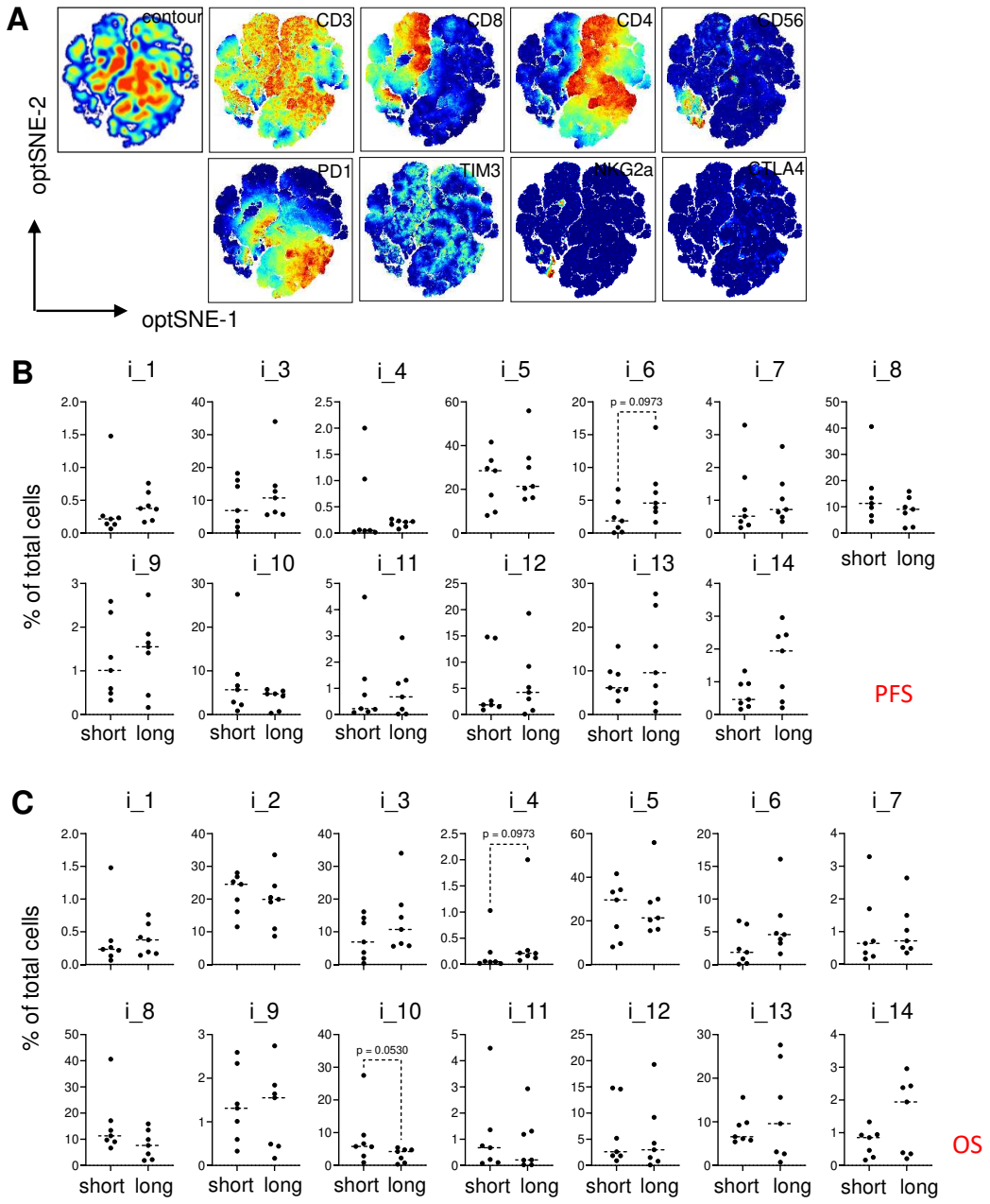

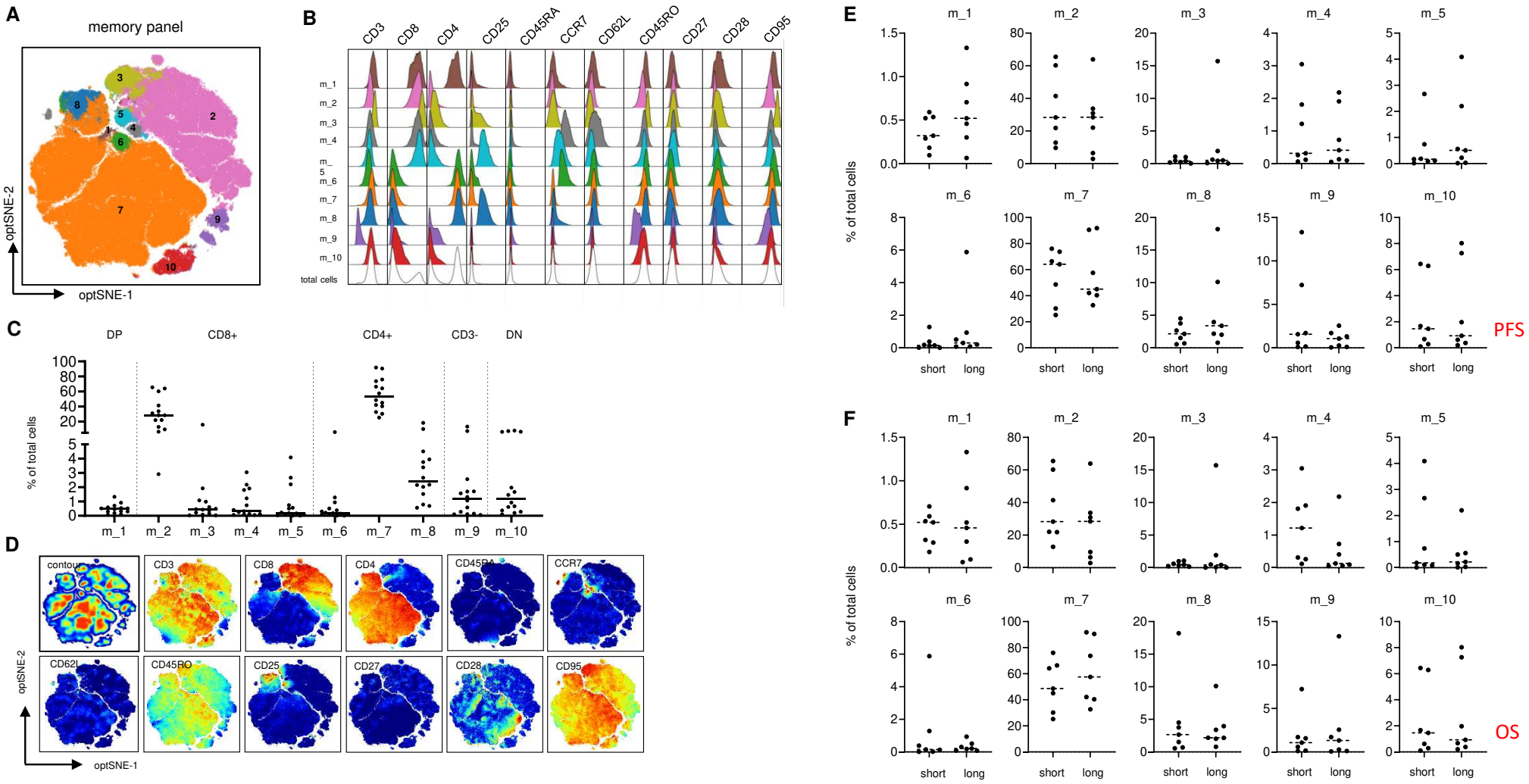

Supplemental Figure S3. Immunophenotyping of infused TIL

Administered TIL were stained with antibody panels specific for memory markers (m), see details in supplemental Table 2.(A) Using opt-SNE, FLOWSOM and OMIQ software 10 different clusters (m_1 thru m_10) were defined. (B) Expression levels of each of the indicated markers is depicted for the individual populations. (C) Frequencies of the identified populations in the total TIL populations are shown and grouped on major phenotypic characteristics, shown above the data; DP=double CD4+CD8+ positive and DN=double CD4 and CD8-negative. (D) Contour plots show the staining intensity of the individual markers used. (E) Frequencies of populations m_1 thru m_10 are shown as percentage of total TIL for patients with a shorter (short) or longer (long) than median PFS, respectively. (F) Similarly, frequencies of populations m_1 thru m_10 are shown as percentage of total TIL for patients with a shorter (short) or longer (long) than median OS, respectively. No statistical differences were observed by Mann-Whitney.

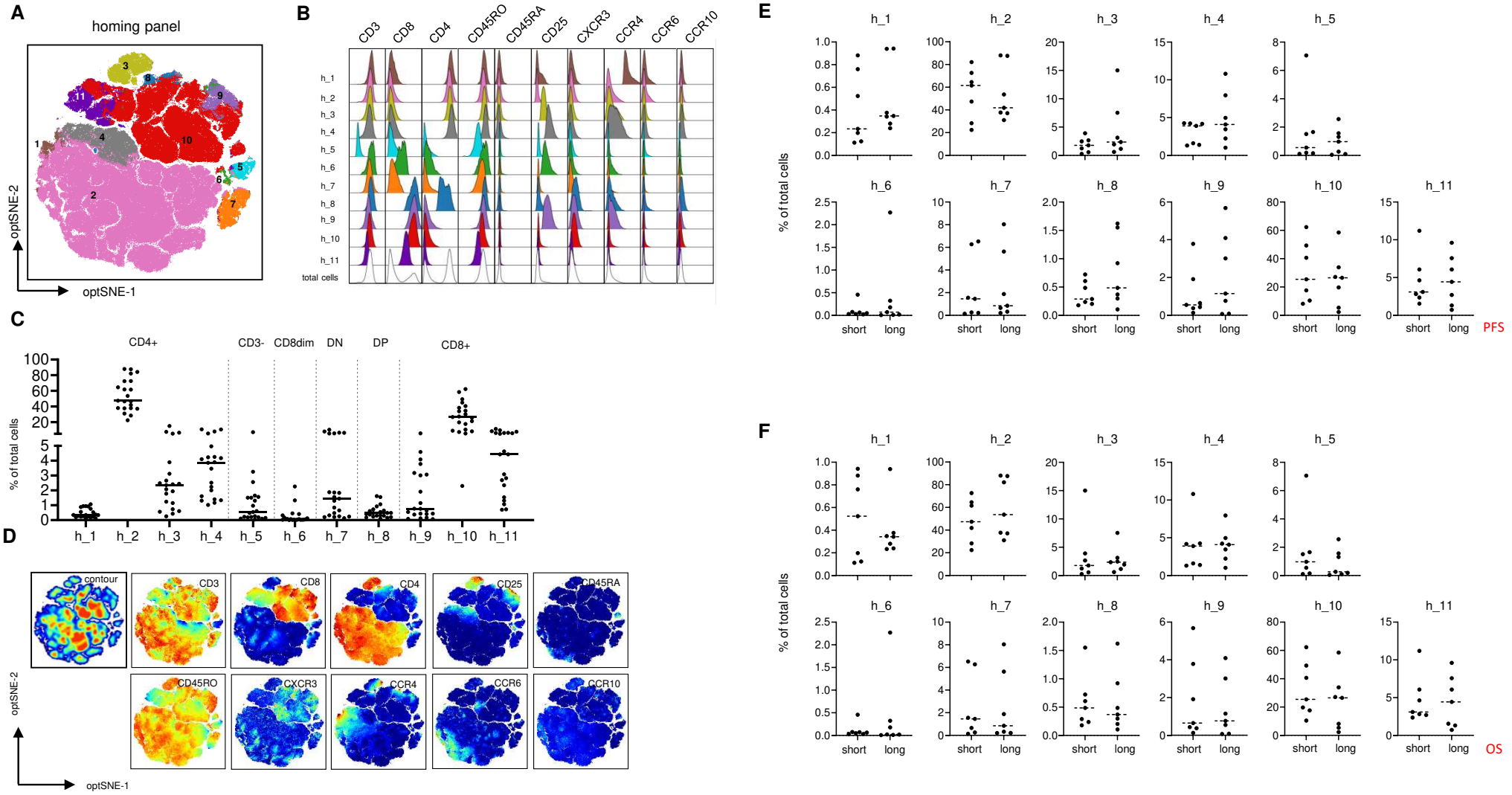

Supplemental Figure S4. Immunophenotyping of infused TIL

Administered TIL were stained with antibody panels specific for homing (h) markers, see details in supplemental Table 2.(A) Using opt-SNE, FLOWSOM and OMIQ software 11 different clusters (h_1 thru h_11) were defined. (B) Expression levels of each of the indicated markers is depicted for the individual populations. (C) Frequencies of the identified populations in the total TIL populations are shown and grouped on major phenotypic characteristics, shown above the data; DP=double CD4+CD8+ positive and DN=double CD4 and CD8-negative. (D) Contour plots show the staining intensity of the individual markers used. (E) Frequencies of populations h_1 thru h_11 are shown as percentage of total TIL for patients with a shorter (short) or longer (long) than median PFS, respectively. (F) Similarly, frequencies of populations h_1 thru h_11 are shown as percentage of total TIL for patients with a shorter (short) or longer (long) than median OS, respectively. No statistical differences were observed by Mann-Whitney.

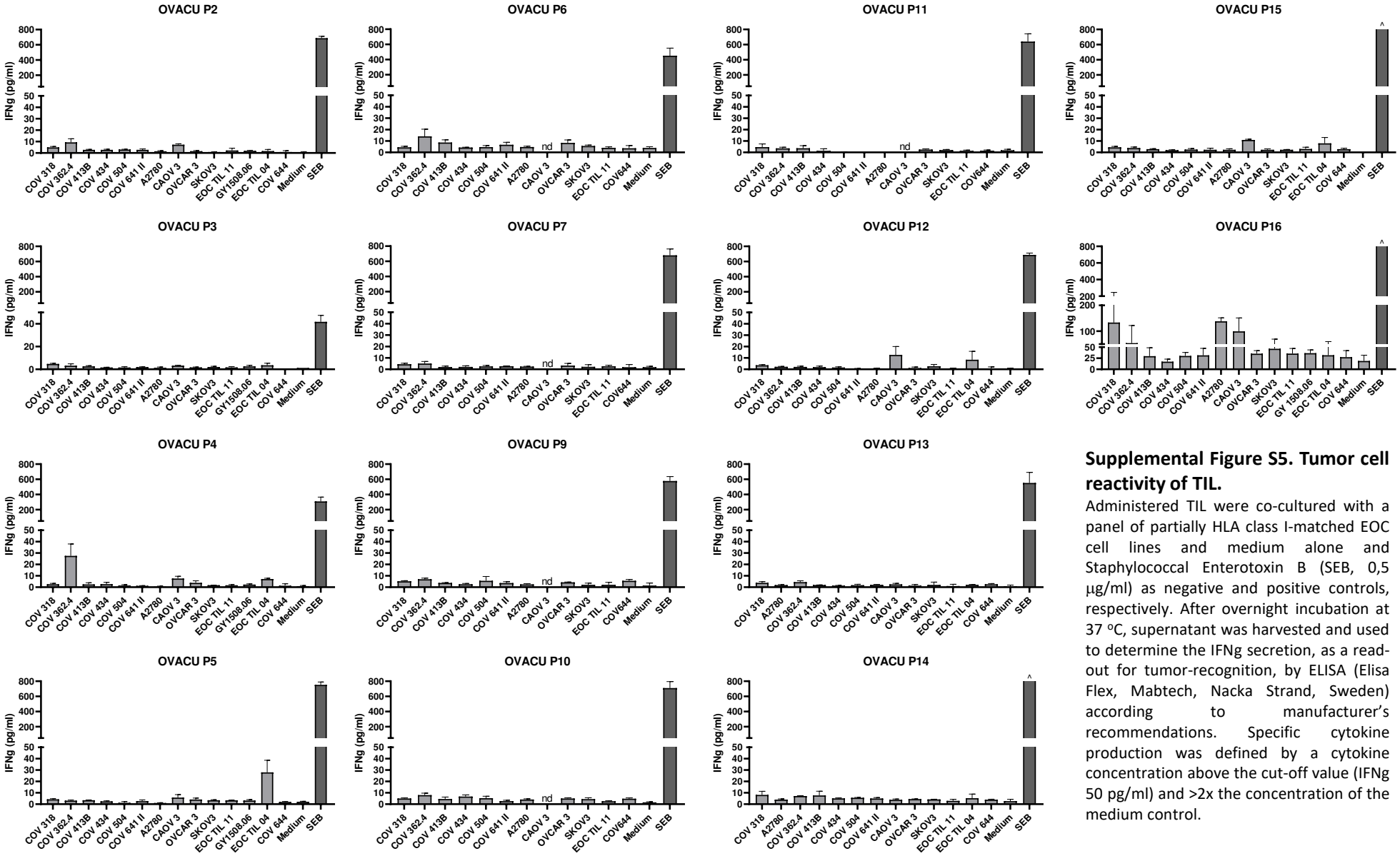

Supplemental Figure S5. Tumor cell reactivity of TIL.

Administered TIL were co-cultured with a panel of partially HLA class I-matched EOC cell lines and medium alone and Staphylococcal Enterotoxin B (SEB, 0,5 µg/ml) as negative and positive controls, respectively. After overnight incubation at 37 °C, supernatant was harvested and used to determine the IFNg secretion, as a read-out for tumor-recognition, by ELISA (Elisa Flex, Mabtech, Nacka Strand, Sweden) according to manufacturer's recommendations. Specific cytokine production was defined by a cytokine concentration above the cut-off value (IFNg 50 pg/ml) and >2x the concentration of the medium control.

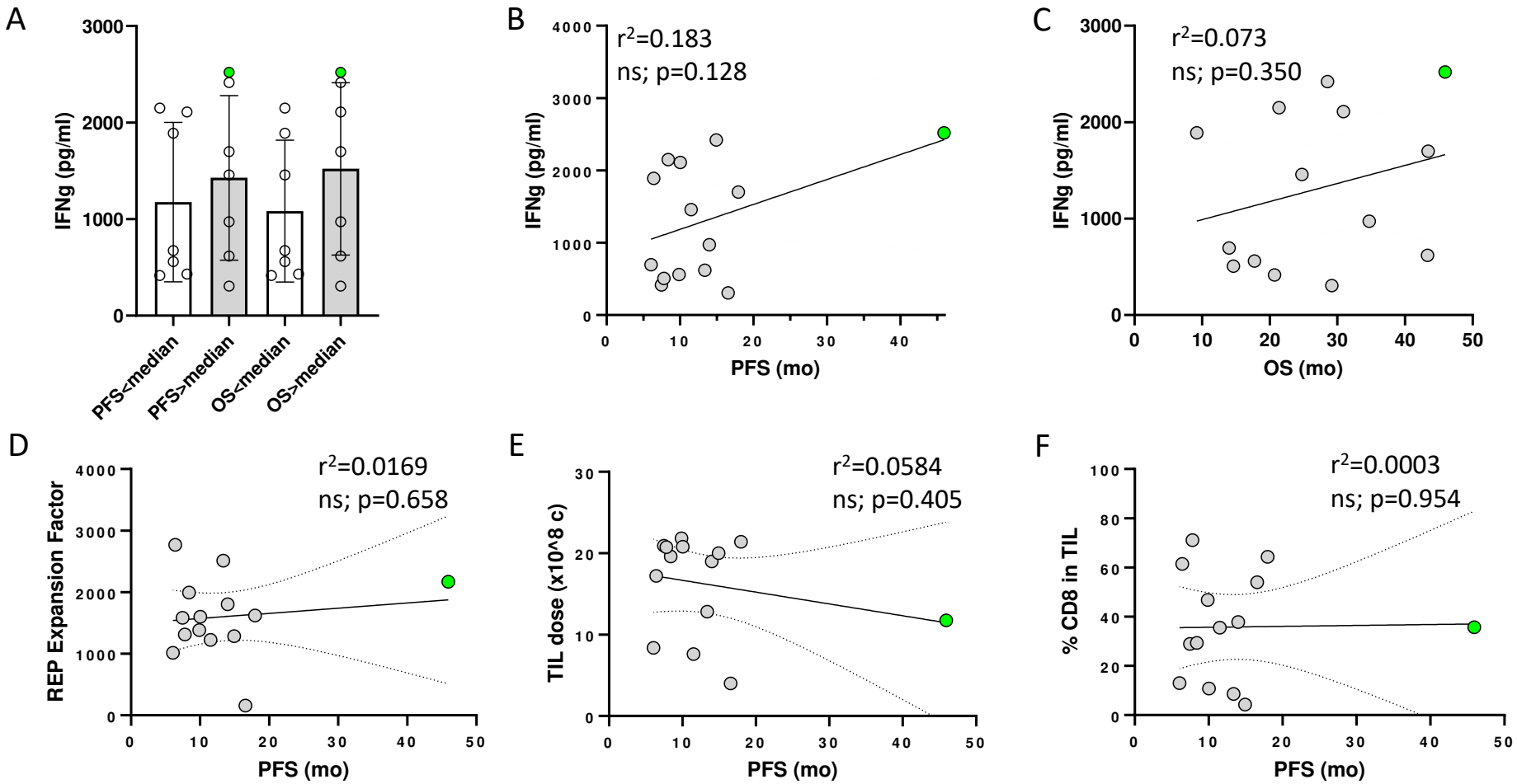

Supplemental Figure S6. Potential Th1 cytokine IFNg production by TIL

Administered TIL were stimulated with CD3/CD28 activation beads (Dynabeads, Thermofisher ratio 1:4 beads to T cells) or medium alone as negative control to assess their potential release of the Th1 cytokine IFNg. After overnight incubation at 37 ^{o}C, supernatant was harvested and used to determine the IFNg production by ELISA (Elisa Flex, Mabtech, Nacka Strand, Sweden) according to manufacturer's recommendations. (A) The specific IFNg production in response to activation beads minus the background is depicted for patients with a shorter or longer than median PFS and OS, respectively. No statistical difference was observed by Mann-Whitney. (B-F) The correlation between IFNg production by stimulated TIL batches and corresponding PFS (B) and OS(C), and correlation between PFS and the TIL expansion factor during the rapid expansion phase (D), the total dose of TIL administered (E), and the percentage of CD8+ T cells in the infusion product (F) were assessed by linear regression analysis using Graphpad software. No significant correlations were found. The dots in green represent patient P6, who experienced a durable CR after treatment.

Supplemental Figure S7. Treatment effect on lymphocyte and APC function.

Treatment effect on circulating lymphocyte and antigen presenting cell function was assessed in peripheral blood mononuclear cells isolated from venous blood samples collected at the indicated time-points before and during treatment. The proliferative response of lymphocytes to (A) influenza M1 (Flu) antigen, (B) memory recall mix (MRM) and (C) CD3/CD28 activation beads, was measured by ^{3}H-thymidine incorporation. The changes are depicted as the proliferation index. (D-F) The APC function was evaluated using a mixed lymphocyte reaction (MLR), results are shown as stimulation index for all patients in (D) and for patients with a shorter (E) and longer (F) than median PFS, respectively. The grey areas indicate the period when the 3 consecutive TIL infusions were administered. Results for the patient with a durable CR (P6) are depicted in green. Significant changes from baseline; *p<0.05; **p<0.01 by paired mixed effects analysis with Geisser-Greenhouse correction.

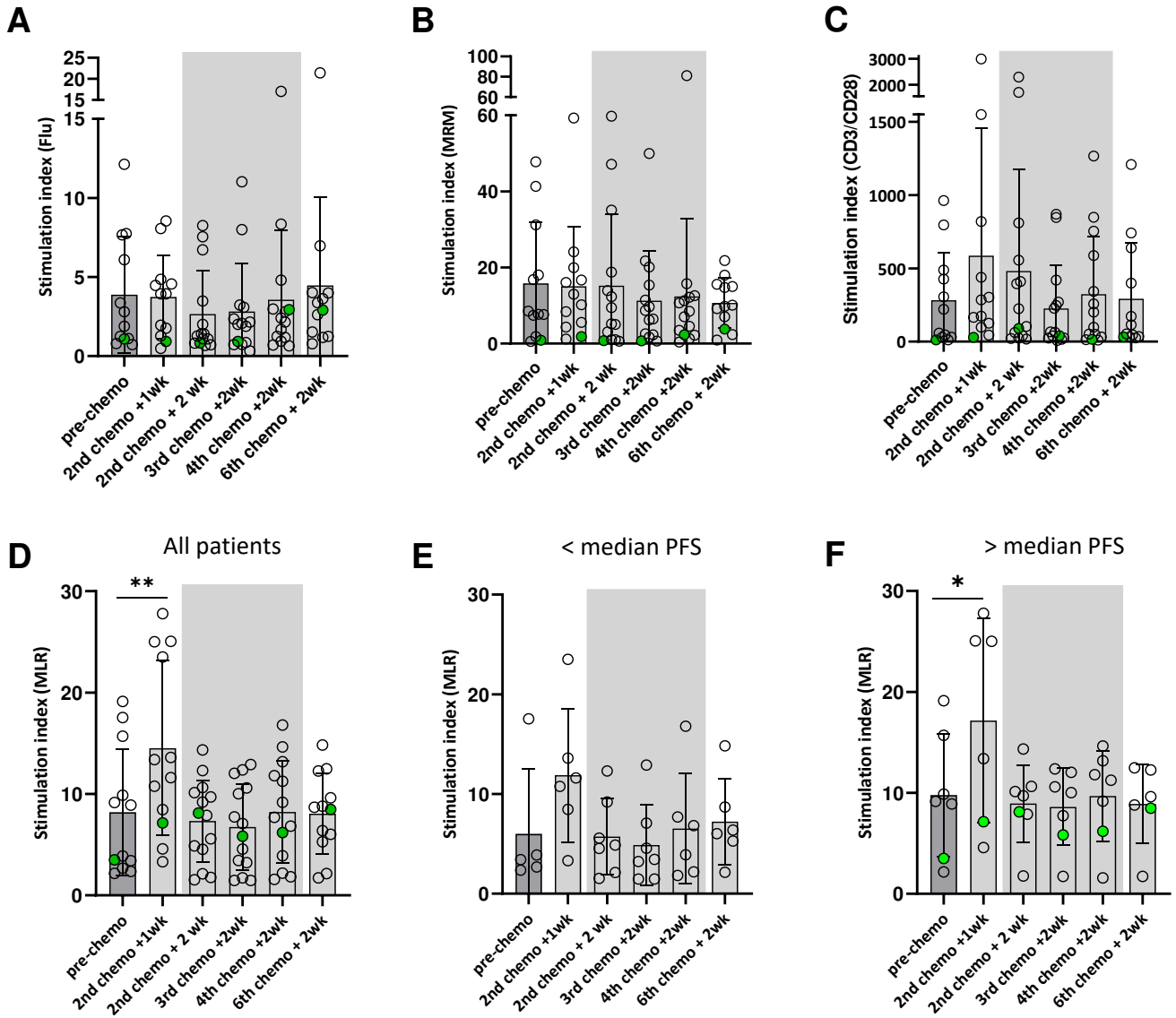

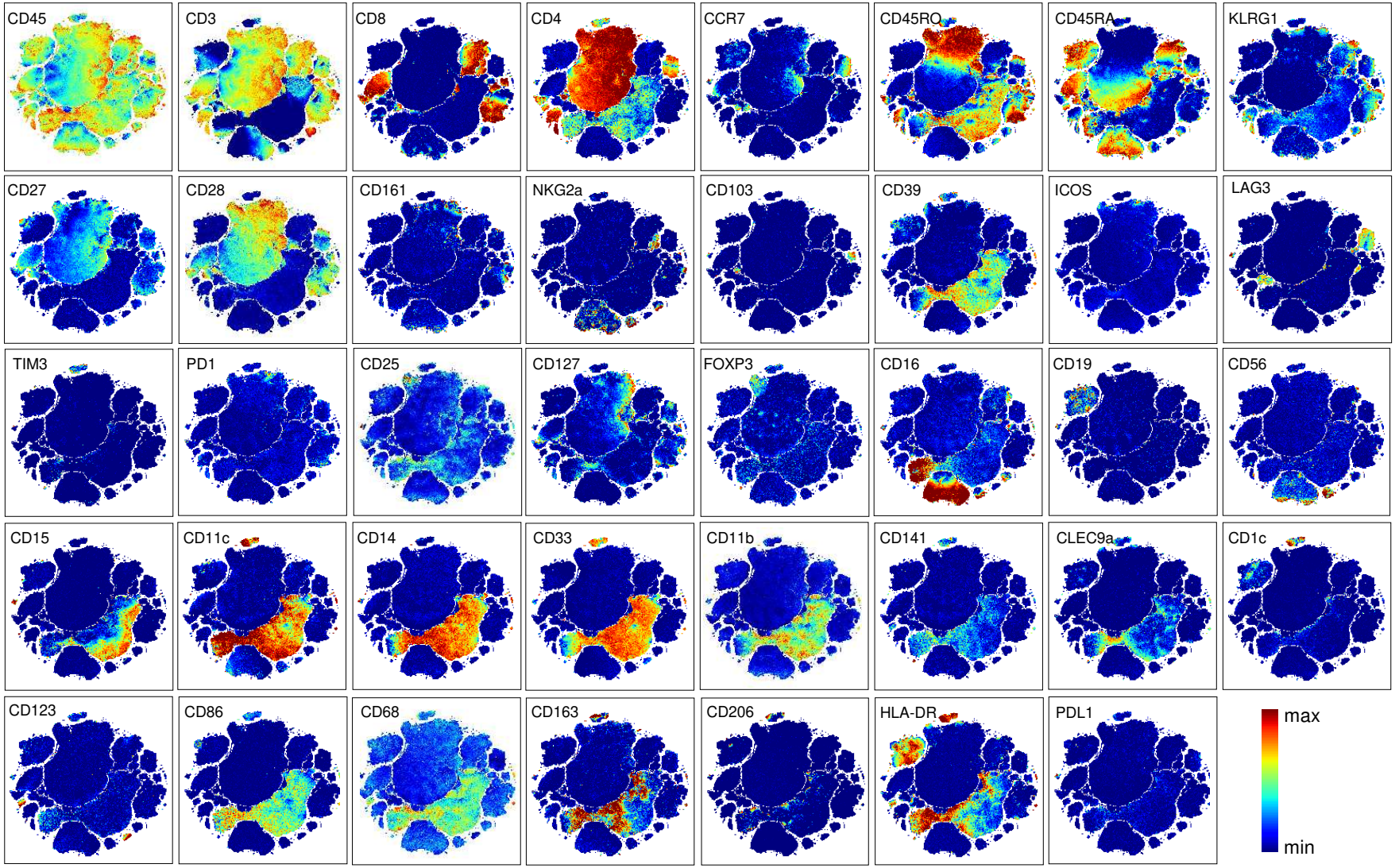

Supplemental Figure S8. Immunophenotyping of PBMC. PBMC isolated from venous blood samples collected at various time-points before and during treatment were stained with a panel of 40 markers (see supplementary Table 1). High-dimensional single cell data analysis of the stained PBMC were performed by opt-Distributed Stochastic Neighbor Embedding (optSNE) and FLOWSOM using OMIQ. Expression levels of each of the indicated markers is depicted in the different panels where red represents maximal and blue minimal staining intensity.

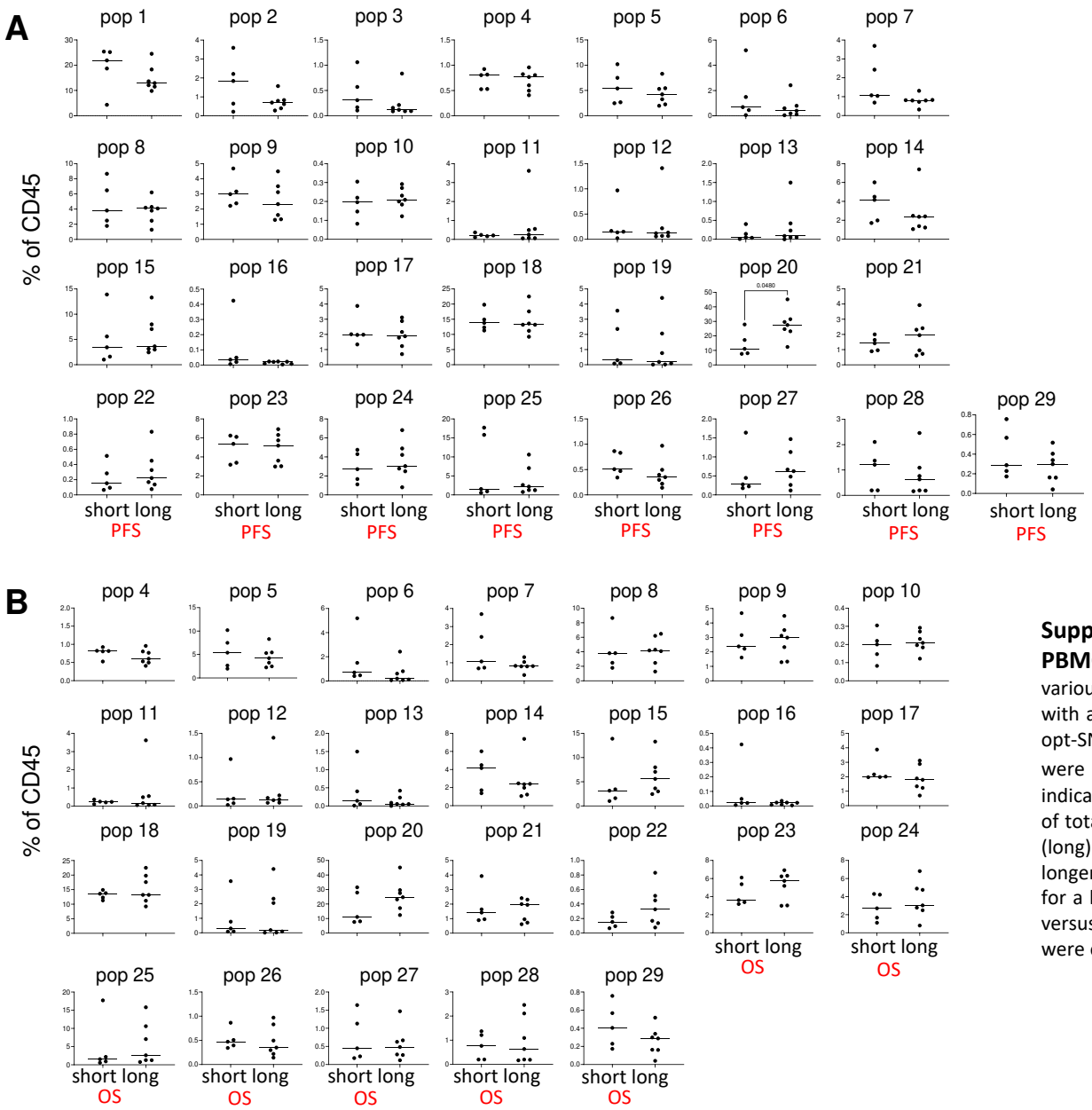

Supplemental Figure S9. Immunophenotyping of PBMC. PBMC isolated from venous blood samples collected at various time-points before and during treatment were stained with a panel of 40 markers (see supplementary Table 1). Using opt-SNE, FLOWSOM and OMIQ software 29 different clusters were defined (see main text Figure 4). Frequencies of the indicated cell populations at baseline are shown as percentage of total CD45+ cells for patients with a shorter (short) or longer (long) than median PFS (upper panels, A), and shorter and longer than median OS (lower panels, B), respectively. Except for a higher frequency of population 20 in patients with longer versus shorter than median PSF, no other statistical differences were observed when analyzed by Mann-Whitney.

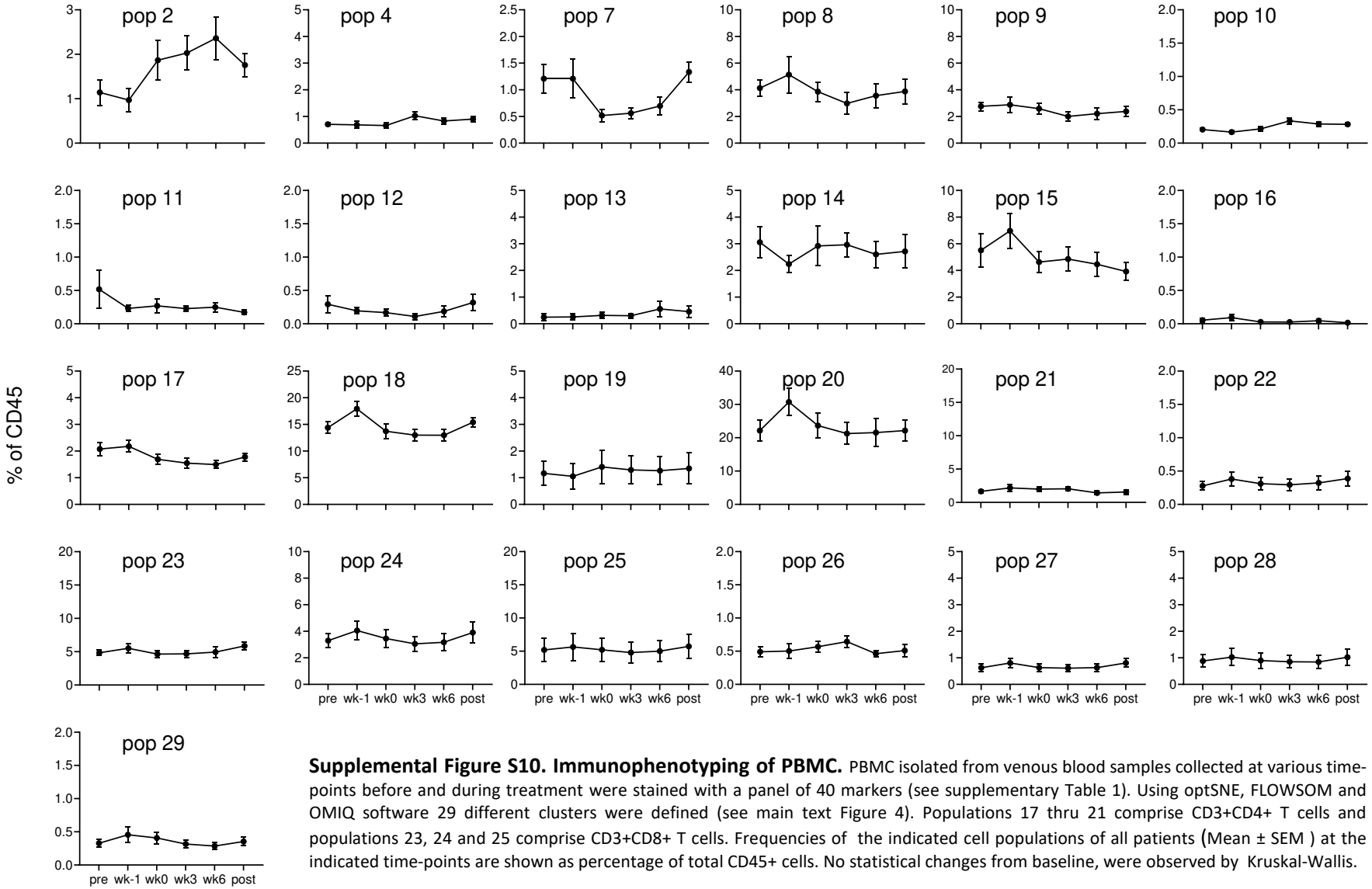

Supplemental Figure S10. Immunophenotyping of PBMC. PBMC isolated from venous blood samples collected at various time-points before and during treatment were stained with a panel of 40 markers (see supplementary Table 1). Using optSNE, FLOWSOM and OMIQ software 29 different clusters were defined (see main text Figure 4). Populations 17 thru 21 comprise CD3+CD4+ T cells and populations 23, 24 and 25 comprise CD3+CD8+ T cells. Frequencies of the indicated cell populations of all patients (Mean ± SEM) at the indicated time-points are shown as percentage of total CD45+ cells. No statistical changes from baseline, were observed by Kruskal-Wallis.